Effect of Ca^{2+} diffusion on the time course of neurotransmitter release

H. Parnas, G. Hovav, and I. Parnas
The Otto Loewi Center for Cellular and Molecular Neurobiology and the Department of Neurobiology, The Hebrew University of Jerusalem, 91904 Israel

ABSTRACT The three-dimensional (3D) diffusion model of Fogelson, A. L., and R. S. Zucker (1985. *Biophys. J.* 48: 1003–1017) has been employed as the basis of a refined version of the "Ca theory" for neurotransmitter release. As such, it has been studied here as to its ability to predict the time course of release under various conditions. In particular, conditions were chosen in which the temporal variations in intracellular Ca^{2+} concentration, the sole factor controlling the release according to the Ca theory, were modified and tested experimentally. The predictions of this model were compared with the experimental results. It is shown that the 3D diffusion model, similarly to earlier simpler versions of the Ca theory, predicts that the time course of release is highly sensitive to both the level of depolarization and the level of the resting concentration of intracellular Ca^{2+} Moreover, the 3D diffusion model predicts that the time course of release is insensitive to changes in temperature. In contrast, the experimental results show that the time course of release is invariant to the level of depolarization and to the resting level in intracellular Ca^{2+}, but highly sensitive to variations in temperature.

INTRODUCTION

The evoked release of neurotransmitter requires the presence of calcium in the external medium. Throughout the years, evidence has been accumulated to suggest that it is the elevation in intracellular Ca^{2+} concentration that triggers the evoked release (Katz and Miledi, 1968, 1977; Llinas et al., 1981; Miledi, 1973). Consequently, the "Ca theory" for evoked release was proposed. This theory postulates that Ca^{2+} is both necessary and sufficient in evoking the secretion of neurotransmitter.

An immediate difficulty that arises from this postulate concerns the different time courses of release after a single pulse and that of facilitation, which presumably results from residual Ca^{2+} (Katz and Miledi, 1968). While the first lasts ~1-2 ms at room temperature, facilitation can last several hundred milliseconds. To account for the above and other difficulties, several hypotheses have been advanced. All are refinements of the Ca theory (Stockbridge and Moore, 1984; Fogelson and Zucker, 1985; Simon and Llinas, 1985). The common postulates for these hypotheses are: (*a*) Ca^{2+} is the only limiting factor in determining release, and (*b*) Ca^{2+}, once entered, diffuses to and away from the release sites. The initial fast diffusion of Ca^{2+} away from the release sites enables for the termination of the evoked release, whereas the later slower diffusion can account for the time course of facilitation.

A different approach, extension of the Ca theory to include an additional limiting factor in release, has recently been suggested (Dudel et al., 1983; Parnas, H., and Segel, 1984; Parnas, H., et al., 1986*a* and *b*). The other factor, similar to the entry of Ca^{2+}, is voltage dependent. Hence, the extended theory was termed the "Ca voltage hypothesis." The essence of this theory is that both Ca^{2+} and another voltage-dependent parameter are required for inducing release. Therefore, Ca^{2+} is essential but insufficient to evoke release. Moreover, the average amount of transmitter being released per pulse, the quantal content, depends on both the concentration of intracellular Ca^{2+} and of that other parameter. The time course of evoked release, on the other hand, is mainly determined by the time course of the latter (Parnas, H., et al., 1986*a*; Parnas, I., et al., 1986).

Several lines of experiments served to support the Ca voltage hypothesis. A detailed account of these experiments is summarized in various publications (Parnas, I., and H. Parnas, 1986; Parnas, I., and H. Parnas, 1988; Parnas, H., and I. Parnas, 1989). Here, some of the key results are briefly mentioned.

The time course of evoked release, as measured by synaptic delay histograms (Katz and Miledi, 1965*a*), was found to be insensitive to modulations in intracellular Ca^{2+} concentration. Thus, the time course remained unaltered when extracellular Ca^{2+} was completely replaced by Sr^{2+} (Datyner and Gage, 1980). It was insensitive to repetitive stimulation (Barrett and Stevens, 1972; Datyner and Gage, 1980; Parnas, H., et al., 1986*a*; and see Fig. 3 here), and it remained the same upon application of a Ca^{2+} ionophore, in spite of a large increase in the quantal content (unpublished results).

The synaptic delay histograms were found, however, to

0006-3495/89/05/859/16 $2.00

be sensitive to some changes in membrane potential. In particular, a short hyperpolarizing postpulse shifted the peak of the delay histogram to the left with a concomitant shortening of the histogram (Parnas, I., et al., 1986; Dudel, 1984*a*). This result is of particular interest in view of the invariance of the time course of release in the face of conditions that alter intracellular Ca^{2+} concentration.

It has been claimed that the above mentioned experimental results do not require one to postulate that Ca^{2+} alone is insufficient for evoking release. Modifications of the classical Ca theory to include details concerning the spatio-temporal behavior of intracellular Ca^{2+} near the release sites were claimed to account for the experimental results that seemed difficult to accomodate in the framework of the classical Ca theory (Stockbridge and Moore, 1984; Fogelson and Zucker, 1985; Simon and Llinas, 1985).

In the present work, we examine one of the most sophisticated of these models, that of Fogelson and Zucker (1985), which we refer to as the 3D diffusion model. We find that this model cannot account for the body of experimental results concerning the time course of evoked release. Moreover, we find that the reason for the difficulties of this refined Ca theory remains, as for the classical one, the postulate that Ca^{2+} is the only limiting factor for release. The 3D diffusion model suffers from an additional problem; diffusion of Ca^{2+} towards and away from the release sites is the key process in determining the time course of release. Consequently, the present model, contrary to experiments, predicts high sensitivity of the time course of release to variations in intracellular Ca^{2+} concentration, but invariance to temperature.

In a subsequent paper (Hovav, G., H. Parnas, and I. Parnas, manuscript in preparation), we show that the 3D diffusion model also fails to account for the experimental results concerning facilitation.

METHODS

As mentioned in the introduction, two key assumptions characterize the 3D diffusion model: (*a*) Ca^{2+} is the only limiting factor for release, and (*b*) diffusion, together with Ca^{2+} influx, is the key process in regulating the spatio-temporal concentration of intracellular Ca^{2+}, and hence, the time course of release. The experiments presented below are oriented towards examining these assumptions.

The deep abdominal extensor muscles of the lobster *Panulirus penicilatus* were used. Recordings were made from the neuromuscular junction of the L_1 muscles (Parnas, I., and Atwood, 1966). Experimental details have been published elsewhere (Parnas, H., et al., 1986*b*). Recordings of synaptic currents were made by the "macropatch" technique (Dudel, 1981). The macropatch electrode had an internal diameter of 10 μm and an external diameter of 20 μm. The same electrode was used to depolarize the nerve terminal and to record synpatic currents (Fig. 1). Data was stored on digital tape (Neurocorder Dr-484, Neuro Data Instrument Corp., New York, NY) at 20 μs/adress. Delay histograms were determined using an Olivetti computer (20 μs/adress). The accuracy of the measurements allowed for a bin size of 0.1–0.2 ms. Saline solution was composed of 520 mM NaCl, 12 mM KCl, 12 mM $CaCl_2$, and Tris maleate 10 mM. pH was adjusted to 7.4. 10^{-7} M TTX was used to block nerve activity.

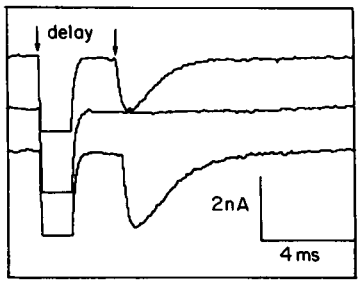

FIGURE 1 Samples of synaptic currents (single quanta) recorded from the L_1 muscle. TTX, 10^{-7} M. Temperature, 14°C. Pulse duration and amplitude, 1 ms and -0.8 μA, respectively. Note failure in release in the middle trace.

EXPERIMENTAL RESULTS

Fig. 2 shows synaptic delay histograms for twin pulses at two levels of depolarization (-0.8 μA and -1 μA). The raw, unnormalized delay histograms are shown in Fig. 2, *a*(-0.8 μA) and *b*(-1 μA). The time interval between the twin pulses (15 ms) was chosen to ensure a complete decay of the release of the first pulse, yet facilitation of the second. The results in Fig 2, *a* and *b*, indeed show that the quantal content, and hence the height of the histogram for the second pulse (*solid line*), is higher than the first for both depolarizations. While the release caused by the second pulse is larger in amplitude, its time course is the same as that of the first pulse (*dashed line*). This is illustrated in Fig. 2, *c* and *d*. Here, the normalized delay histograms of the two pulses are superimposed. It can be seen that both curves overlap at the two levels of depolarization.

The effect of depolarization on the time course of release is illustrated in Fig. 2 *e*. On the left side of this figure, the normalized delay histograms of the first pulses at the two levels of depolarization are superimposed. It is apparent that increasing depolarization (dashed line) did not alter the time course of release. In particular, release did not start earlier, the time of the peak was the same, and the duration of release was not changed. These conclusions are substantiated in the results on the right side, where the second pulse of the two depolarizations is shown. Fig. 2 *e* illustrates an additional aspect which concerns facilitation. To demonstrate this, the following procedure of normalization has been employed. The delay

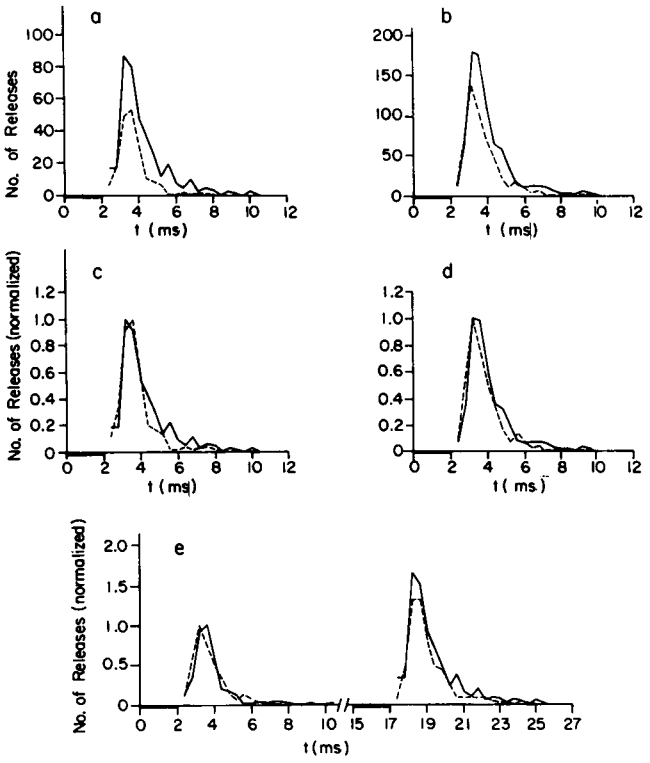

FIGURE 2 Synaptic delay of twin pulses at two levels of depolarization. (*a*) Delay histograms of the first (*dashed line*) and the second (*solid line*) pulses at -0.8 μA. (*b*) As in *a*, but for -1 μA. In *c* and *d*, the first and the second pulse of *a* and *b* are normalized to their peak amplitude. (*e*) On the left side, the first pulses of the -0.8 μA (*solid line*) and the -1 μA (*dashed line*) are normalized, each to its peak amplitude. On the right side, the second pulse of each of the depolarizations is normalized to the peak amplitude of its first pulse. Notice that the lower depolarization (*solid line*) shows higher facilitation. Temperature of 10°C. Normal Ringer + 10^{-7} M TTX. The continuous lines are obtained by taking the middle time point of a 0.4-ms bin. 1,000 2-ms pulses were employed in each histogram. The quantal contents were: 0.20, 0.41, for the first and second pulses in *a*, and 0.65, 0.82 for the first and second pulses in *b*.

histogram of the second pulse at each level of depolarization has been normalized to the peak amplitude of its first pulse (Fig. 2 *e, right*). In this way, the dependence of facilitation (in addition to the dependence of the time course) on depolarization could be examined. (Facilitation is discussed in detail in a subsequent paper [Hovav, G., H. Parnas, and I. Parnas, manuscript in preparation], however relevant information is extracted from the present experiment.) Fig. 2 *e, right,* shows that facilitation decreases as depolarization is raised.

Together, the results of Fig. 2 suggest that the time course of release is independent of depolarization and also insensitive to the level of intracellular calcium concentration that exists before stimulation. It could be claimed, however, that the latter results from insufficient accumulation of calcium. We therefore compared delay histograms of a test impulse and that of the last impulse in a train of five impulses. The results are depicted in Fig. 3. It is apparent that even though the quantal content increased from 0.11 to 0.7, release elicited by the fifth impulse did not start earlier than that elicited by the test impulse. A longer tail release is seen after the train. In other such experiments, even the duration of release was not altered (Datyner and Gage, 1980; Parnas, H., et al., 1986*a*).

The last experiment was designed to determine whether or not diffusion of calcium, toward and away from the release sites, determines the time course of release, in particular, the minimal latency and the decay. Toward this end, we examined the dependence of the time course of release on temperature. Fig. 4, *A–C*, shows delay histograms obtained at 9 ± 0.5°C and 19 ± 0.5°C. At the higher temperature, 800 pulses were given at a rate of 2 Hz. The pulse duration was 0.5 ms, and its amplitude was -1.2 μA. 235 quanta were released, and the quantal content was thus 0.27. The preparation was rapidly cooled to 9°C, and a pulse of 0.5 ms duration was given. At this pulse duration, only eight quanta were released for 1,000 impulses. This finding shows that the quantal content in the lobster neuromuscular junction is very sensitive to changes in temperature with a Q_{10} of 34. At this pulse duration, the number of quanta was too small to construct a delay histogram. Therefore, we have prolonged the pulse to 0.7 ms. Here, 81 quanta were released per 1,150 pulses. At a 1-ms duration, 348 quanta were released for 1,900 impulses at 2 Hz. The delay histograms given in Fig 4 for the two temperatures are composed of the same

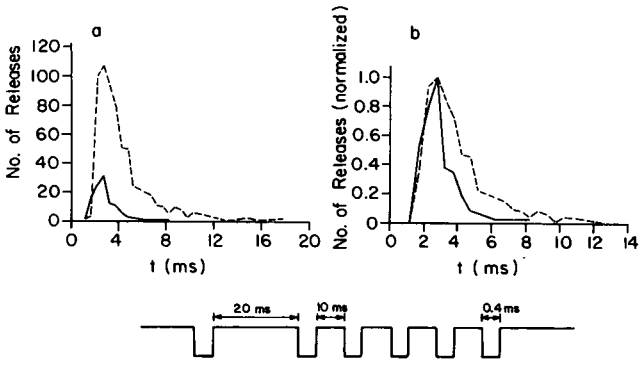

FIGURE 3 Synaptic delay histograms elicited by a test impulse (*solid line*) and by the last impulse in a train of five impulses (*dashed line*). A test pulse of 0.4 ms and -1.2 μA was followed 20 ms later by a train of five impulses, 10 ms apart. Repetition rate was ½ s. 1,000 such repetitions were given. The quantal content of the test impulse was 0.11, and that of the last pulse of the train, 0.7.

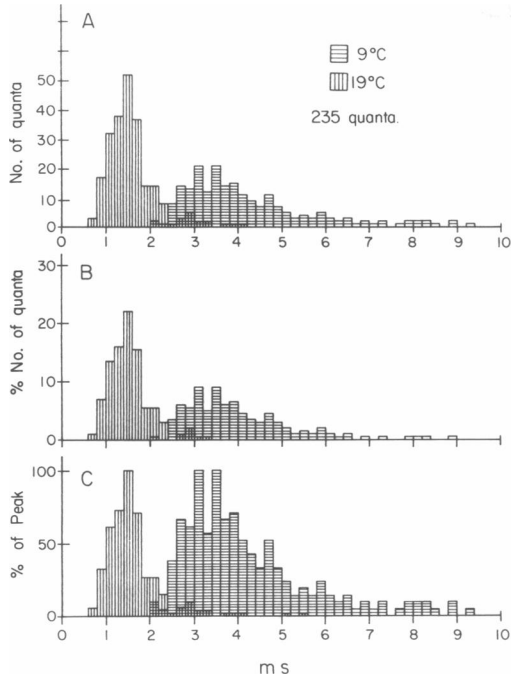

FIGURE 4 Delay histograms established at 19°C (*horizontal bars*) and 9°C (*vertical bars*). For each delay histogram, 235 quanta were taken. At 9°C, the first 235 quanta of 348 were taken. (*A*) Number of quanta released per bin. (*B*) The values at each bin given as percentage of the 235 quanta. (*C*) Normalization to the peak value. The delays were measured at 20 μs/adress and bin width was taken as 0.2 ms. At 19°C, 800 pulses were given and 235 quanta observed. At 9°C, 1,900 pulses were given and 348 quanta obtained. Pulse parameters: 19°C, 0.5 ms, −1.2 μA. 9°C, 1 ms, −1.2 μA. Normal Ringer, 2.10^{-7} TTX.

number of quanta, 235. The histograms are given in absolute values (Fig. 4 *A*), as a percentage of the total number of quanta (Fig. 4 *B*), and normalized to the peak (Fig. 4 *C*). In this experiment, the Q_{10} of the minimal delay was 3.3. In seven other experiments, the Q_{10} for the minimal latency varied between 3 and 4.5. These values are in the range of Q_{10} values found in other preparations (Katz and Miledi, 1965*b*; Dudel, 1984*b*). It is also evident that other aspects of the delay histogram, such as amplitude and time to peak, are sensitive to temperature.

The aspects of the experimental results can be summarized as follows. (*a*) Release starts after the end of a 2-ms depolarizing pulse (at 8–11°C). This result is not altered by changing either the level of depolarization, or the level of intracellular calcium before stimulation. (*b*) The rate of release reaches its maximum significantly after the end of the depolarizing pulse. In particular, for a 2-ms pulse, release reaches its peak at ~4 ms. (*c*) The time course of release is independent of the level of depolarization during the pulse, and does not depend on the resting level of intracellular calcium. In particular, the minimal latency, the time of the peak, and the duration of release (under the conditions presented in Fig. 2), were not altered when either depolarization or the resting level of intracellular calcium were modified. (*d*) The time course of release is highly sensitive to temperature. In particular, the minimal latency shows a Q_{10} larger than three.

Note that the insensitivity of the delay histogram to variations in depolarization and to the resting level of intracellular calcium (result 3) reflects a genuine property of the release process. It does not result from technical limitations in detecting small changes. As mentioned in Methods, even changes as small as a shift of 0.2 ms in the delay histogram can be detected.

In the following, the 3D diffusion model will be compared with the experiments presented above, and also with similar experimental results which appear in the literature.

Presentation of the 3D diffusion model

We first present the equations of the 3D diffusion model, and later, our procedure for solving these equations. Let $C(x, y, z, t)$ be the concentration of free calcium above the resting level in a rodlike unit element of the presynaptic terminal (Fig. 5). Here, x, y, and z are the space coordinates, and t denotes time. The temporal change in $C(x, y, z, t)$ at any point inside the unit element (excluding the membrane surface) is given by the three-dimensional diffusion equation

$$\frac{\partial C}{\partial t} = \frac{D}{1+B}\left[\frac{\partial^2 C}{\partial x^2} + \frac{\partial^2 C}{\partial y^2} + \frac{\partial^2 C}{\partial z^2}\right], \qquad (1)$$

where D is the diffusion coefficient for calcium in aqueous solution, and B is the ratio of bound to free calcium.

At the membrane surface, i.e., at $y = Y_0$, the following boundary conditions are assumed to hold:

$$D \cdot \frac{\partial C}{\partial y} + P \cdot C = f(x, z) \cdot g(t) \qquad \text{at } y = Y_0. \qquad (2a)$$

Here, P stands for a rate constant of a pump that extrudes Ca^{2+}. Note that the rate of pumping is linear with the Ca^{2+} concentration. The function $f(x, z)$ in Eq. 2a describes the distribution of the Ca channels that will open in the patch of the membrane under consideration (see Fig. 5). Because the channel mouth is relatively small in comparison to the patch, $f(x, z)$ is the sum of deltalike functions that are centered on the channels. Also in Eq. 2a, $g(t)$ describes the time course of opening of the channels. g is zero when the channels are closed, and takes on a positive value when the channels are opened. At that time, the diffusive flux $\partial C/\partial y$ in Eq. 2a is determined

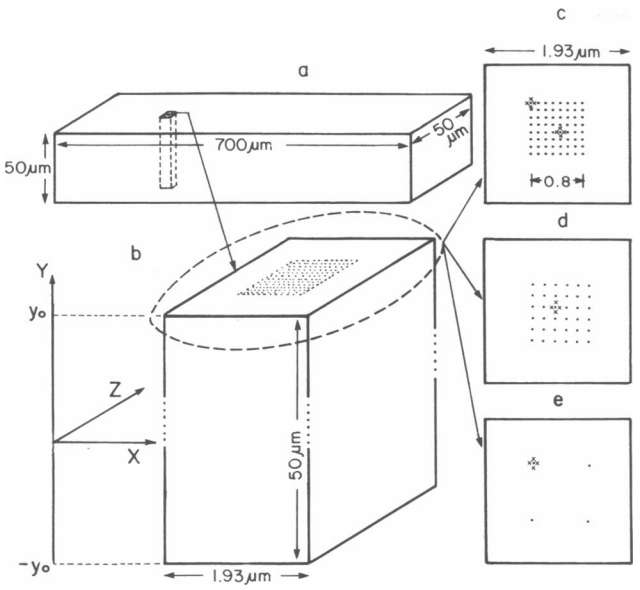

FIGURE 5 The presynaptic cell is represented by a box. (*a*) The cell membrane with its active zone (i.e., the area that includes the Ca^{2+} channels and the release sites) is located on the upper surface of the box. The computation unit is depicted in *b*. An enlargement of the active zone is seen in the circle in *b*. Inside, the Ca^{2+} channels are illustrated as dots. The length of the channel array is 0.8 μm. The three standard depolarizations are: 0 mV, or above (*c*), will be denoted as high depolarization. In this case, 64 channels in the active zone are opened. Hence, the distance between pairs of opened channels is 0.1 μm. The corresponding value of g is 0.5. Medium depolarization corresponds to −15 mV (*d*). Then, 36 channels are opened. Hence the distance between pairs of opened channels is 0.16 μm. The value of g in this case is taken to be 0.8. Finally, low depolarization corresponds to −25 mV (*e*). In this case, only four channels are opened, the distance between pairs of opened channels is 0.44 μm, and $g = 1$. In this standard model, the release sites are situated at a distance of 0.05 μm from a channel, and each channel is surrounded by four release sites. The values of the above listed parameters were extracted from Table 1 in Zucker and Fogelson (1986). The values of the rest of the parameters (Eqs. 1–5) that compose the standard model are $D = 0.6\ \mu m^2/ms$ (Hodgkin and Keynes, 1957); $P = 0.08\ ms^{-1}$; $B = 500$; $n = 4$; $k = 1$. The function f is taken as in Fig. 7 *c*. $g = 0$ when the channels are closed, and positive when they are open.

both by the influx of Ca^{2+} (i.e., $f(x, y)$) and by its extrusion by means of the pump (i.e., $P \cdot C$). When $g = 0$, only the pump affects the flux.

The model also describes the situation at the opposite membrane, at $y = Y_0$, where

$$-D \cdot \frac{\partial C}{\partial y} + P \cdot C = 0 \qquad \text{at } y = -Y_0 . \tag{2b}$$

The difference between Eqs. 2a and 2b is due to the absence of channels on the membrane at $y = -Y_0$. Eq. 2b is of no real importance, because under most conditions, almost no Ca^{2+} that enters at Y_0 reaches $-Y_0$.

A further assumption in the 3D diffusion model is that there is no diffusion across the boundaries of the model element (i.e., at $\pm X_0$ and $\pm Z_0$). Thus,

$$\frac{\partial C}{\partial x} = 0 \text{ at } x = \pm X_0 \quad \text{and} \quad \frac{\partial C}{\partial z} = 0 \text{ at } z = \pm Z_0 . \tag{3a and b}$$

The initial condition for C is that

$$C(x, y, z, 0) = 0 \qquad \text{at } t = 0 . \tag{4}$$

Note that Eq. 4 implies that the resting level of intracellular Ca^{2+}, before the first pulse, is zero.

Finally, the rate of release of neurotransmitter, R, is proportional to the nth power of C at a given release site. Hence,

$$R(x, z, t) = K \cdot C^n(x, Y_0, z, t) . \tag{5}$$

From Eq. 5, it follows that the release sites are located at the surface membrane, where the Ca^{2+} channels are also embedded.

Solution of Eqs. 1–5

Fogelson and Zucker solved Eqs. 1–5 analytically. To achieve this goal, flexibility of the model was sacrificed. For example, as previously mentioned, the entry of Ca^{2+} is described by a rather arbitrary nonphysiological function, $f(x, z)$. Also, both the pump (Eq. 2a) and the release (Eq. 5) were described by nonsaturating functions.

In the present work, we examine the 3D diffusion model for its ability to predict a wide range of experimental results. This requires a higher degree of flexibility than that which can be achieved by use of the analytical solution of Eqs. 1–5. We therefore employed numerical solutions (Crank, 1975). Unfortunately, we had to retain the unnatural entry of Ca^{2+}, because it comprises one of the major elements of the Fogelson-Zucker model.

Our procedure for solving Eqs. 1–5 is described below, as well as in Fig. 5. Following Fogelson and Zucker, the dimensions of the square membrane patch in the basic computation element were taken to be 1.93 μm in length, and 50 μm in depth. This element was divided into small cubes of 0.0193 μm length. Hence, the element can be considered as an ensemble of layers at different distances from the surface membrane. Each layer contains 100 · 100 cubes. For this element, the procedure of solution is as follows. The first step involves solution of Eq. 1 with the aid of the following (conventional) finite difference approximations:

$$\frac{\partial^2 C}{\partial x^2} \approx \frac{1}{dy^2} \cdot (-2 \cdot C[x, y, z, t] + C[x + dx, y, z, t] + C[x - dx, y, z, t]), \tag{6a}$$

$$\frac{\partial^2 C}{\partial y^2} \approx \frac{1}{dy^2} \cdot (-2 \cdot C[x, y, z, t] + C[x, y + dy, z, t] + C[x, y - dy, z, t]), \quad (6b)$$

$$\frac{\partial^2 C}{\partial z^2} \approx \frac{1}{dz^2} \cdot (-2 \cdot C[x, y, z, t] + C[x, y, z + dz, t] + C[x, y, z - dz, t]). \quad (6c)$$

The concentration of calcium, C, at a given interval point at time $t + dt$, is obtained by incorporation of Eq. 6 into Eq. 1. Thus,

$$C(x, y, z, t + dt) \approx C(x, y, z, t) + \frac{dt \cdot D}{1 + B}\left(\frac{\partial^2 C}{\partial x^2} + \frac{\partial^2 C}{\partial y^2} + \frac{\partial^2 C}{\partial z^2}\right). \quad (7)$$

This procedure is repeated for any interval of time. Sufficiently small time intervals were chosen to assure convergence of the solution.

The concentration of calcium at the surface membrane is obtained by a numerical solution of Eq. 2a. Thus,

$$\frac{\partial C}{\partial y} \approx \frac{C(x, Y_0, z, t) - C(x, Y_0 - d\,y, z, t)}{dt}. \quad (8a)$$

Incorporation of Eq. 8a into Eq. 2a and rearrangement gives

$$C(x, Y_0, z, t) \approx \frac{g(t) \cdot f(x, z) \cdot dy + C\,(x, Y_0 - dy, z, t)}{1 + dy \cdot P/D}. \quad (8b)$$

Note that when the channels are closed so that $g(t) = 0$, Eq. 8b is simplified to

$$C(x, Y_0, z, t) \approx \frac{C(x, Y_0 - dy, z, t)}{1 + dy \cdot P/D}. \quad (8c)$$

Examination of Eq. 8c shows the relative importance of both the pump and the diffusion in regulating the intracellular calcium concentration.

As mentioned earlier, we solved Eqs. 1–5 by a different procedure than that used by Fogelson and Zucker (1985). Therefore, it is important to show that the two procedures can produce similar results. To this end, we repeated one of the most basic experiments, the spatio-temporal changes in C at low and high depolarizations. The results are depicted in Fig. 6. One can see that at short times, C is concentrated below the channels (curves 1 and 2 in Fig. 6, *c* and *d*). Later, as C diffuses, its concentration becomes more uniform in the vicinity of the channels (curves 3 and 4 in Fig. 6, *c* and *d*). The effect of increased depolarization is seen in Fig. 6 *c*. Due to the high density of opened channels, C also accumulates in regions that are some distance from any particular channel. The corresponding results of Zucker and Fogelson (1986), under the same conditions, are shown in the upper part. Fig 6 *a* depicts the results for high depolarization and Fig. 6 *b* for low depolarization. It can be seen that the two solution procedures give identical results.

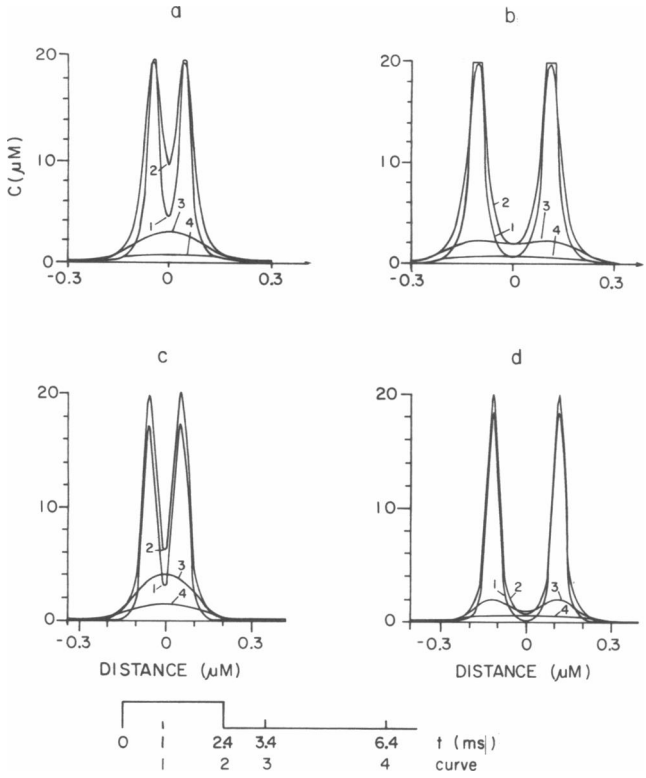

FIGURE 6 Simulation of the spatio-temporal variation in C below the membrane at two levels of depolarization under two channels. The curves represent the spatial distribution of C at various times from the beginning of the pulse. The scheme at the bottom relates the number at each curve to the corresponding time. Redrawing of the analytic results of Zucker and Fogelson (1986) is seen in *a* and *b*, whereas the results of our numerical solution of Eqs. 6–8 are shown in *c* and *d*.

Behavior of the 3D diffusion model in view of experimental results

We now examine the ability of the 3D diffusion model to correctly predict the time course of release at conditions where the dynamics of intracellular Ca^{2+} concentration is varied.

Effect of the f function

Because this model depends heavily on the *f* function, it is important to show the effect of this function on some aspects of release. This is shown in Fig. 7. Three representative examples were chosen. In the first example, upon opening of the channels, the membrane is regarded as

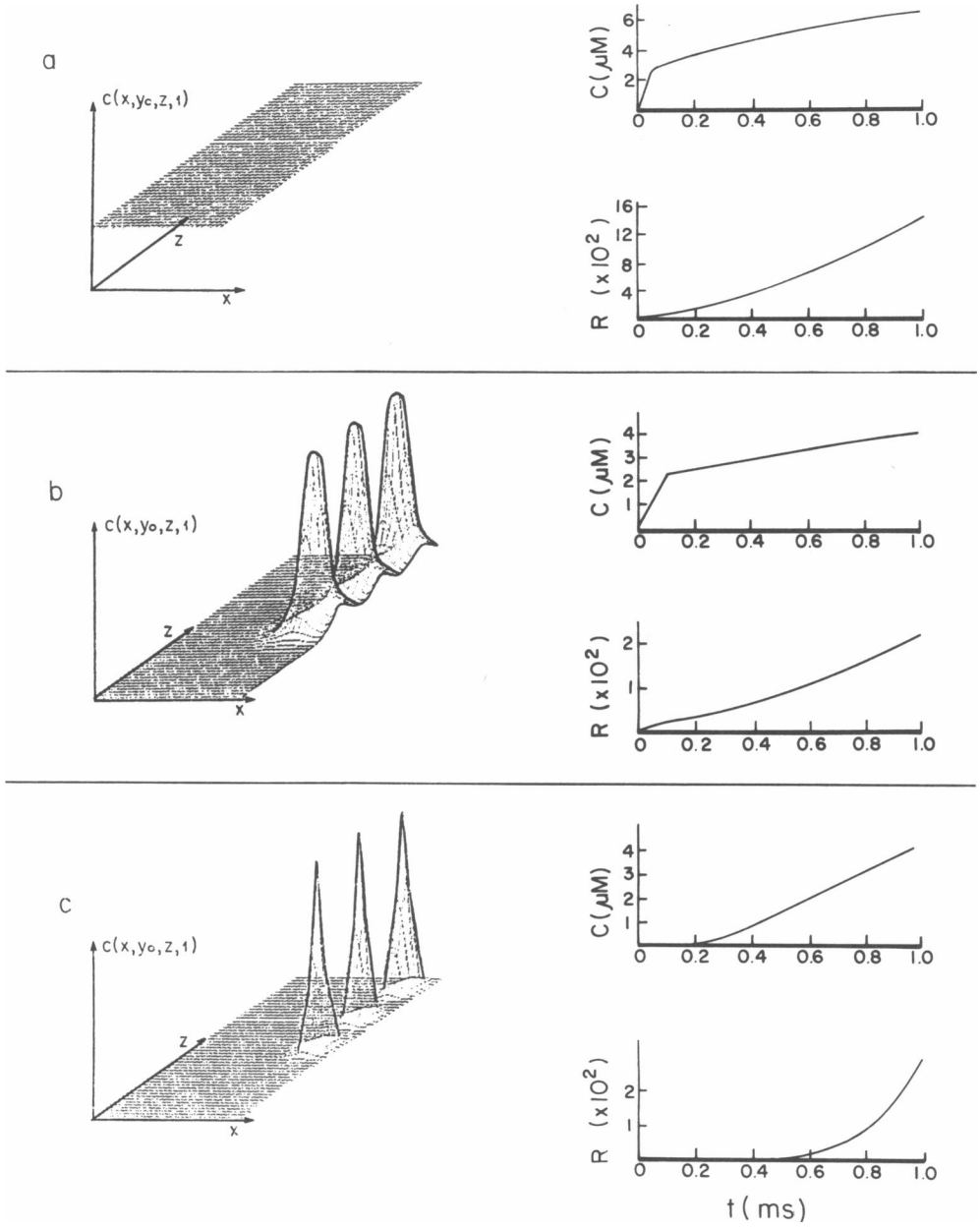

FIGURE 7 The dependence of C and R on the nature of the f function. The spatial distribution of C at the end of a 1-ms pulse is depicted on the left side. Note that C, below and around three channels, is seen in *b* and *c*. The temporal variations in C (at the release site) and in R during the pulse are shown on the right side. (*a*) $f(x, z)$ = constant. (*b*) $f(x, z) = \Sigma_i f_i(x, z)$, where i is an open channel. Here, $f_i(x, z) = K_f \exp\{d[(x, z), (x_i, z_i)]/2\sigma^2\}$, where (x_i, z_i) denote the location of the ith open channel, $\sigma = 0.16$, and $K_f = 550$. The distance between the (x, z) spot and the ith open channel is given by $d[(x, z), (x_i, z_i)] = [(x - x_i)^2 + (z - z_i)^2]^{1/2}$. f in b is thus the sum of deltalike functions approximated by a Gaussian function. Note that even though (unlike *a*), each individual channel is represented and the distance between the channels is 0.16 μm, the temporal behavior of C (on the right) is similar to that in *a*. The reason is that $f(x, z)$ is not very steep. (*c*) $f(x, z)$ as in (*b*), but $\sigma = 0.1$. This case also differs from *b* in that here, if $d[(x, z), (x_i, z_i)] < r$, then $f_i(x, z) = 0$. Thus r determines the localization of the source of the "influx" of calcium. Note that this mild modification of $f(x, z)$ results in a significant alteration of C, and hence of R.

uniformly leaky (Fig. 7 *a*) and release R, in this case, starts without delay. Another $f(x, z)$ is shown in Fig. 7 *b*. There, some C is accumulated near the channels as soon as they open. In this case, similar to that in Fig. 7 *a*, release R starts immediately. Finally, in Fig. 7 *c*, $f(x, z)$ is a very narrow and steep Gaussian function. This results in a highly localized increase in C just below the channel (Fig. 7 *c*). Consequently, the predicted delay histogram, R, shows a lag before the rate of release starts to rise. Obviously, there is no direct experimental way to assess which of these possibilities is closer to reality. In the following, we adopted case 7 *c*. The reason for this choice is that only this possibility is capable of producing a latency before release starts, as observed experimentally (see Figs. 2–4). Moreover, this f function was employed by Fogelson and Zucker (1985).

We define the "standard model" to include $f(x, z)$ of Fig. 7 *c*, parameters that concern the various depolarizations as in Fig. 5, and values for the various parameters associated with Eqs. 1–5. The latter are also listed in the legend of Fig. 5.

Dependence of the time course of release on temperature

In the 3D diffusion model, the time course of release depends on the diffusion of Ca^{2+} to and away from the release site. In particular, the minimal latency (the time that elapses between the pulse and the beginning of release) is governed by the time that it takes C to diffuse from the channel to the release sites. Furthermore, the decay of release is determined by diffusion of C away from the release sites. These aspects are illustrated in Fig. 8. Here, the release site was located at a distance of 50 nm (Fig. 8, *a* and *c*) and 100 nm (Fig. 8, *b* and *d*) from a channel. Low depolarization was employed to avoid overlaping effects of C from the various open channels. It can be seen that as the release site is moved further away from the channel, the minimal latency increases. The latency increased from ~0.4 ms, when the site was located 50 nm from an opened channel (Fig. 8 *c*), to ~1.2 ms, when the site was moved to be 100 nm from an opened channel. Note also the much lower C that reaches the release site in the more distant location (compare Fig. 8, *b* and *a*). Consequently, the decay of release at the more distant site is much slower.

In conclusion, Fig. 8 shows that the minimal latency, the time of peak release, and the decay of release are governed by diffusion. Hence, the model predicts that the whole time course of release depends very weakly on temperature.

In contrast, experiments show that the minimal latency, as well as the entire time course of release, strongly depend on temperature (Katz and Miledi, 1965*b*; Barrett and Stevens, 1972; Dudel, 1984*b*; and see Fig. 4).

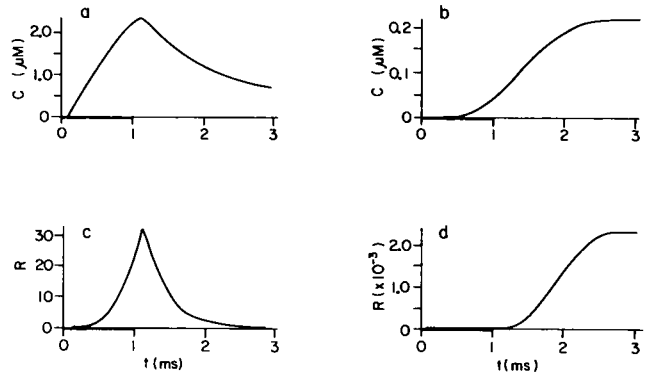

FIGURE 8 Simulation of C and R at two locations of the release site. The time course of C at the release site is shown when the release site is at a distance of 50 nm (*a*) and 100 nm (*b*) from the channel. The corresponding values of R are shown below. Note that the level of C is 10 times lower at the more distant site and its time course is different. The peak amplitude of C is obtained at the end of the pulse in *a*, but only 1 ms later at the more distant site at b. The corresponding values of R show the same variations in time course. Release starts 0.2 ms from the beginning of the pulse at the nearer site and reaches its peak amplitude at the end of the pulse. However release starts only after the end of the 1-ms pulse (i.e., at ~1.2 ms) at the more distant site. Here, the low level of depolarization has been employed to avoid overlapping between channels. R of Eq. 5 has been used.

The experimental results suggest that it is not diffusion that governs the time course of release. Later, we will discuss means within the framework of the model to correct this discrepancy.

Time course of release and its dependence on depolarization and the resting level of intracellular Ca^{2+}

Fig. 9 shows the predicted time course of C and the resulting rate of release, R (according to Eq. 5), for twin pulses at two levels of depolarization. The location of the site under investigation is denoted by x in the squares (upper part). Following the 3D diffusion model, the release site is located at a distance of 50 nm from the channel. Some clarification is required when the effect of depolarization is discussed. The 3D diffusion model does not contain a physiological description of the effect of depolarization. Instead, these authors provide a rigid connection between some chosen levels of depolarization and a corresponding density and location of open channels, on one hand, and the driving force per channel, on the other hand (see Table 1, Zucker and Fogelson, 1986). In our attempt to remain close to the original model, we employed the same parameters, as chosen by Fogelson and Zucker, for the two levels of depolarization shown in Fig. 9. These two levels of depolarization (low on the left side and high on the right side) were defined in Fig. 5, and are a part of the "standard model." For each depolariza-

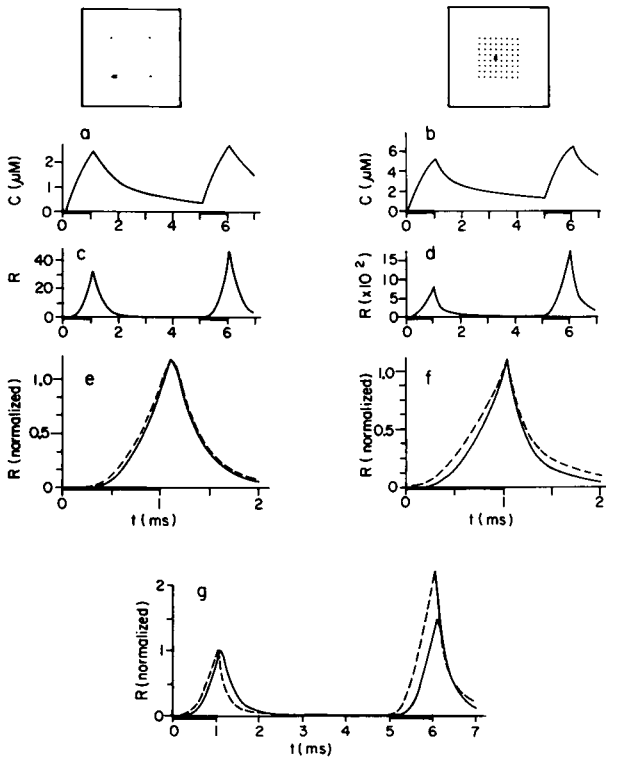

FIGURE 9 Simulation of C and R of twin pulses at two levels of depolarization. The configuration of the open channels and the location of the release site under investigation is depicted in the squares in the upper part. The low depolarization (−25 mV) is shown on the left side, and the high depolarization (0 mV), on the right side. Twin pulses of 1 ms with a 5-ms interval between pulses were employed. The duration of the pulse is shown by a heavy line. C and R of the low depolarization are shown in *a* and *c*, respectively, and C and R of the high depolarization in *b* and *d*, respectively. Superimposed in *e* and *f* are releases elicited by the second (*dashed line*) and the first (*solid line*) pulses at the low (*e*) and the high (*f*) depolarizations, each normalized to its peak amplitude. (*g*) On the left side are superimposed values of R for the first pulses of the low (*solid line*) and high (*dashed line*) depolarizations. Each R is normalized to its peak amplitude. In *g*, on the right side, the procedure of normalization is the same as for the experiments (Fig. 2) to observe facilitation. That means that R, for the second pulse at each depolarization, is normalized to the peak amplitude of its first pulse. The dashed line corresponds to the high depolarization, and the solid line to the low depolarization. Note that facilitation is higher at the higher depolarization. The two levels of depolarization correspond to the low and high depolarization of the "standard model."

tion, two 1-ms pulses with a 5-ms interval between them were employed. The resultant C and R at the low depolarization are depicted in Fig. 9, *a* and *c*, respectively, whereas the C and R of the high depolarization are shown in Fig. 9, *b* and *d*. The protocol of these simulations was chosen to match the experimental conditions (Fig. 2); the second pulse is administered when the release of the first is fully completed, but when facilitation still exists. The latter ensures that the resting level of C is still elevated when the second pulse is administered. In the experiments of Fig. 2, the interval between the twin pulses was 15 ms, whereas it is only 5 ms in the simulations. A closer resemblance between the experimental and simulation conditions is not possible, because in the 3D diffusion model, C drops to very low levels in ~7–10 ms after the first pulse. Moreover, because diffusion is the main reason for this fast removal, lowering the temperature (as done in the experiments) will not improve the situation.

Fig. 9 should be compared with the experimental Fig. 2. Several lines of difference are apparent. Most noticeable are the minimal latency and the time of peak release. In the experiments (Fig. 2), the minimal latency outlasts the duration of the 2-ms pulse. Moreover, release reaches its peak at ~3.5 ms, which is significantly after the end of the 2-ms depolarizing pulse. Both of these results are general findings. Under most conditions, the time of the peak was found to be significantly after the end of the pulse (Katz and Miledi, 1965; Datyner and Gage, 1980; Barrett and Stevens, 1972; Dudel, 1984*a* and *b*; Parnas, H., et al., 1986*a*; Parnas, I., et al., 1986), and remained so, even for pulses as long as 10 ms (Wojtowicz et al., 1987). Because this result is obtained at all levels of depolarization, it cannot be attributed to a late entry of Ca^{2+}. Furthermore, in agreement with the observation in Fig. 2, the minimal latency was found to outlast the duration of the pulse, providing that the pulse is not longer than 2–3 ms Parnas, H., et al., 1986*a* and *b*; Parnas, I., et al., 1986; Wojtowicz et al., 1987; Parnas, H., and Parnas, I., 1987; and see Figs. 2 and 3). This holds for low and moderate temperatures. Contrary to these observations, the model predicts both a minimal latency much shorter than the 1-ms depolarizing pulse, and the peak of release to occur at the end of the pulse (Fig. 9, *c* and *d*).

Another typical difference concerns the duration of release. In Fig. 2, the release lasts ~6 ms, whereas it lasts only <2 ms in the model (Fig.9). The model predicts that about one-half of the release occurs during the pulse, and that the entire release process is too short. In principle, these discrepancies could be corrected by lowering the temperature. Experimentally, lowering the temperature results in prolongation of the minimal latency, shift of the peak of release towards longer delays, and slowing the decay of release (see Fig. 4). However as discussed earlier, in its present form, the model is insensitive to temperature. Hence, lowering the temperature is not expected to reconcile the differences between the experimental Fig. 2 and the theoretical Fig.9.

The dependence of the time course of release on depolarization is depicted in Fig. 9 *g*. It is seen that increasing depolarization (dashed line in Fig. 9 *g*) alters the time course of release. Throughout this work, we have tried to remain as close as possible to the parameters used in the original 3D diffusion model. In particular, we used

the same depolarizations. This resulted in rather small differences in C at the release site. Thus, the peak of C at the low depolarization is ~2.5 μM (Fig. 9 *a*), whereas it is ~5 μM at the high depolarization (Fig. 9 *b*). Despite the rather moderate difference in C, meaningful variations in R are apparent (Fig. 9 *g*). We would like to draw attention to two aspects. First, at the second pulse, the peak amplitude of R is obtained sooner at the higher depolarization (dashed line in Fig. 9 *g*, right side). Second, as judged by the peak amplitude of R, facilitation is higher at the higher depolarization (dashed line). Both of these predictions differ from the experimental results in Fig. 2 *e*. Note, however, that there are no dramatic discrepancies between the experiments and the model concerning the dependence of the time course on depolarization.

It is difficult to assess the predictions of the 3D diffusion model concerning the effect of the resting level of intracellular Ca^{2+} on the time course of release. The reason is that the model does not include a resting level of Ca^{2+} before the first pulse. The effect of the resting level can be elevated indirectly by employing a second pulse at a time when the remaining C from the first pulse is still evaluated. This aspect is also seen in Fig. 9. At the low depolarization, the two normalized curves of the first (solid line) and the second (dashed line) pulses show a very similar time course (Fig. 9 *e*). At the high depolarization, however, the second pulse shows shorter minimal latency and longer duration (Fig. 9 *f*). Note that because the curves are normalized, these results indicate a genuine shortening of the minimal latency, and a genuine prolongation of the decay constant of release. The tendency of shortening the minimal latency and prolongation of release becomes quite obvious when three pulses are employed (Fig. 11). In contrast, the experiments show that the time course of release is invariant to the level of the resting Ca^{2+} concentration. In particular, Fig. 2, *c* and *d*, show that release did not start sooner after the second pulse (solid line), in spite of the higher quantal content after the second pulse (Fig. 2, *a* and *b*). Moreover, even the minimal latency after the fifth pulse remained unaltered, in spite of an increase of sevenfold in the quantal content (Fig. 3).

Modification of the 3D diffusion model

Until now, we analyzed the 3D diffusion model using the original equations and parameters as suggested by the authors. We will now modify some aspects, leaving the kernel of the model unaltered. We chose aspects for modification according to one or both of two considerations. Either an aspect is known to be an oversimplification, and as such is a natural candidate for modification, and/or there are intuitive reasons for believing that a certain modification might correct a defect in the basic model.

Modification of R to be a saturated functions of C

In the present model, the rate of release, R, is assumed to be proportional to the nth power of C, without saturation at higher levels of C (see Eq. 5). Saturation is, however, expected, because it is assumed that Ca^{2+} binds to some entity x, and that this binding (which of course in principle is saturable) starts the chain of events leading to release (Katz and Miledi, 1968). Moreover, there are indirect experimental findings that led Parnas, H., and Segel (1980) to suggest that Eq. 5 should be replaced by a more general saturative equation. Thus,

$$R(x, z, t) = \frac{\bar{R} \cdot C(x, Y_0, z, t)^n}{[K_R + C(x, Y_0, z, t)]^n}, \qquad (9)$$

where $\bar{R}$ denotes the maximal possible release, and K_R denotes a Michaelis-Menten constant. The value of K_R will determine whether or not saturation occurs in the physiological range of C. The quantal content was shown to saturate at physiological concentrations of extracellular Ca^{2+} concentrations (Dodge and Rahamimoff, 1967; Parnas, H., et al., 1982). At the same range of concentrations, facilitation was shown to decline as extracellular Ca^{2+} concentration was raised (Rahamimoff, 1968; Parnas et al., 1982). Based on these findings, it was concluded that release saturates at physiological levels of intracellular Ca^{2+} concentration (Parnas, H., and Segel, 1980; Parnas, H., et al., 1982). Fig. 10 shows the expected dependence of the time course of release on depolarization, where Eq. 9, rather than Eq. 5, is employed. K_R has been given a value that allows saturation of release to occur at the levels of C obtained by the 3D diffusion model.

Note that except for this change, the other conditions are exactly as in Fig. 9. In particular, the levels of depolarization are the same, and hence the C profile is unaltered, yet the time course of release is changed. Two major aspects concerning the time course of release are apparent in Fig. 10. (*a*) Release after the second pulse starts earlier than that after the first (Fig. 10, *e* and *f*). In comparison with Fig. 9 *e*, this trend is now clear, even at low depolarization (Fig. 10 *e*). (*b*) Upon increasing depolarization, release starts sooner, and the time to the peak becomes shorter (Fig. 10 *g*). With the saturated release, this trend becomes apparent, even for the first pulse (see Fig. 10 *g*, left side). The trend toward earlier release in the presence of saturation can be intuitively understood by considering the extreme case. If the rate of release is

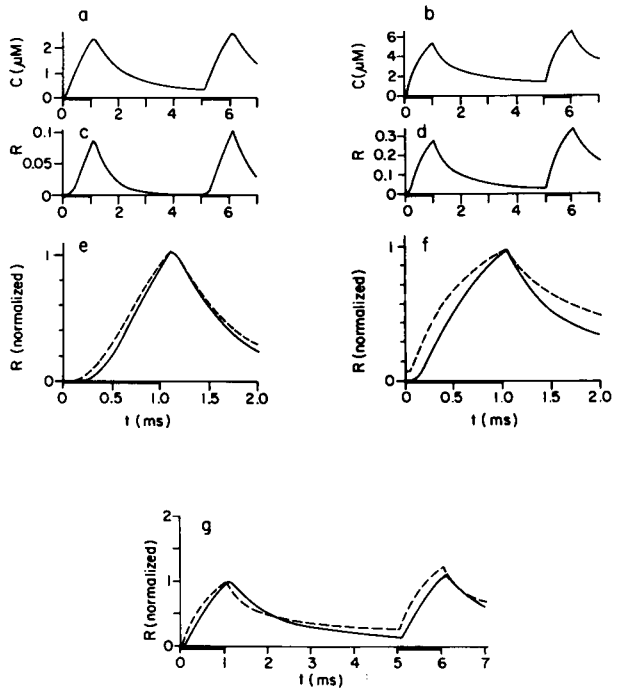

FIGURE 10 C is calculated as in Fig. 9, but R is given by Eq. 9. The parameters of Eq. 9 are $\bar{R} = 1$, $K_r = 2$ μM and $n = 4$. Note that *a* and *b* are identical to *a* and *b* in Fig. 9. However with saturative R, the difference in time course of release elicited by the first (*solid line*) and the second (*dashed line*) pulses is already noticeable for the low depolarization (*e*) and becomes more pronounced at the higher depolarization (*f*). Also, saturation in release emphasizes the differences in the time course of release at the two levels of depolarization (*g*).

fully saturated as a function of Ca, then there will be no need whatsoever to wait for entry to build up the intracellular calcium to cause release to commence.

We observed that the 3D diffusion model predicts that as C builds up, release induced by the same test pulse will start sooner and will last longer (Figs. 9, *e* and *f*, and Fig. 10, *e* and *f*). This tendency becomes even more pronounced when three, rather than two, pulses are employed. Three pulses, at the high depolarization, with a 5-ms interval between pulses, were employed. The results are seen in Fig. 11. The peak level of C was increased from ~5.5 μM after the first pulse to ~7 μM following the third pulse (Fig. 11 *a*). Yet this rather small increase caused a significant change in the time course of release. Even with the unsaturated R, release started with practically zero delay after the third pulse, and its duration was considerably prolonged (Fig. 11 *d*). These results are strongly amplified when a saturated R is employed (Fig. 11 *e*). Here, even the shape of R is altered when successive pulses are employed. It is apparent in Fig. 11 *d*, and more so in Fig. 11 *e*, that the present model predicts, not surprisingly, a continuous release after a longer train of pulses. In contrast, Fig. 3 *b* shows that in the experiments, even the release elicited by the fifth pulse started after exactly the same minimal latency. However in agreement with the model, the duration of release after the fifth pulse was longer than that after the first pulse.

Modification of the model to include slow kinetics of the Ca^{2+} channels

As discussed earlier, the 3D diffusion model predicts that the time course of release is insensitive to variations in temperature. There are three main possibilities for correcting this discrepancy without interference with the main lines of the model. (*a*) The direct calcium regulation processes, diffusion, buffering, and/or pumps can be effected. (*b*) Temperature can modify the opening and closing of Ca^{2+} channels. (*c*) There could exist a temperature-dependent step that links the calcium concentration with exocytosis.

With respect to possibility *a*, it is well known that diffusion constant D is weakly affected by temperature. As for the pumps, they only have a very small effect on the basic 3D diffusion model (otherwise, diffusion would not be the dominant process). Thus, the only way to account for the effect of temperature would be to assume that the pumping rate increased significantly with temperature, but then, the problems mentioned above (Fig. 9 in comparison with Fig. 2) would be made even worse. As for a temperature effect on buffering, we cannot rule this out in principle, but this matter would require a separate study, including, for example, the possibility of abandoning the greatly simplified assumption (used in the 3D diffusion model) that buffering is fast and hence merely affects the diffusion constant.

We now consider possibility (*b*) above, i.e., the kinetics of the Ca^{2+} channels. Because the model does not include implicit kinetics of the Ca^{2+} channels, we modified the g function in Eq. 2a. More specifically, at the "high temperature" (Fig. 9), the g function was described by a square pulse of 1 ms. At the "low temperature," on the other hand (Fig. 12), g is described by a gradual increasing and decreasing function (see lower part in Fig. 12). The depolarizing pulse is still of a 1-ms duration, but g reached its maximal value only at the end of the pulse, and then declined gradually instead of abruptly. Note that at this lower temperature (Fig. 12), the build-up of C is more gradual (Fig. 12, *a* and *b*). Consequently, similar to the experiments, the minimal latency almost outlasts the length of the pulse. This improvement becomes less profound for the second pulse at the higher depolarization (Fig. 12 *f*, dashed line). Also, at the lower temperature, the sensitivity of the time course of release to depolarization is more apparent. Fig. 12 *g* (right side) shows that in contrast to experiments, at the higher depolarization (dashed line), release starts significantly earlier, and the

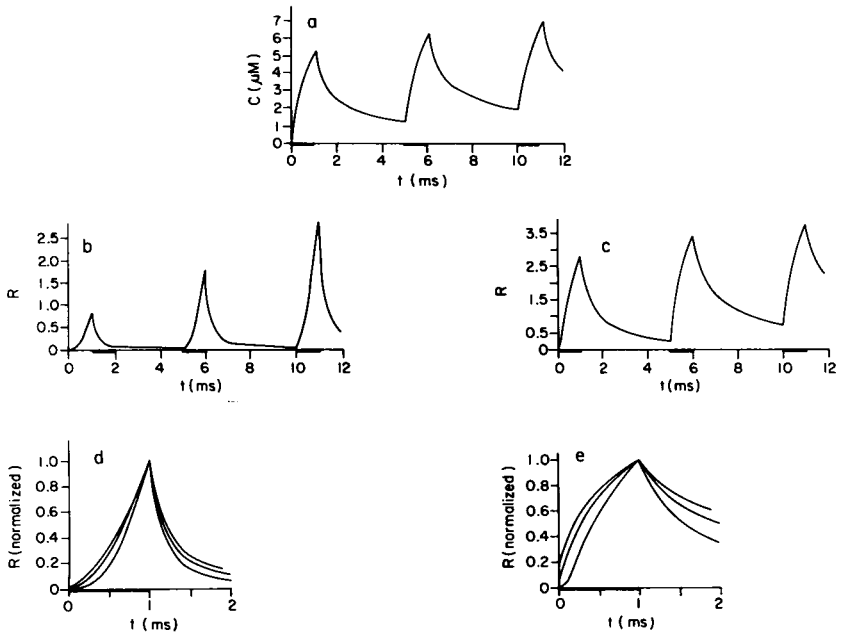

FIGURE 11 Simulation of C and R in a train of three pulses. The three pulses of C are depicted in *a*. *b* and *c* illustrate the corresponding values of R using Eqs. 5 and 9, respectively. *d* and *e* Three superimposed curves of R, each normalized to its peak amplitude when R is given by Eqs. 5 and 9, respectively. The high level of depolarization was employed.

facilitation of the second pulse is much higher at the higher depolarization. Finally, slowing the kinetics of "opening" and "closing" the Ca^{2+} channels shifted the release towards longer delays but failed to slow down the decay of release. The duration of the release process in this lower temperature remained 2–4 ms (Fig. 12) too short in comparison with the experimental results (Figs. 2 and 4).

Modification of the model to include a slow step after the entry of Ca^{2+}

A third possibility for causing the time course of release to become sensitive to temperature (possibility *c*) is to include a slow process that links Ca^{2+} to exocytosis. Such a modification (like the previous one) does not alter the essence of the Ca theory. Ca^{2+} still remains the sole necessary and sufficient parameter for evoking release. Moreover, various experimental results support the notion that the slowest process in release is not associated with either entry or removal of Ca^{2+}. For example, curare has been found to alter the time course of release. In particular, it delayed the peak of release and its decay without affecting any aspect that concerns the temporal change in intracellular Ca^{2+} concentration (Matzner et al., 1988).

We then leave the kernel of the model unaltered. That is, C is determined as before, but instead of R being just proportional to C^n (Eq. 5), we write the minimal model that has been suggested by Katz and Miledi (1968) and Dodge and Rahamimoff (1967). The kinetics of this model are as follows:

$$C + X \underset{k_{-1}}{\overset{k_1}{\rightleftharpoons}} Q, \qquad nQ \xrightarrow{k_2} R \qquad \text{(10a and b)}$$

where X is an unknown site to which Ca^{2+} must bind to start the chain of events leading to release, R. In Eq. 10, X is constant so that only C determines the time course of R. It should be mentioned that when C is the only limiting factor for release, identical results are obtained from the model in Eq. 10 and from a similar variation of it in which the kinetics are given by

$$nC + X \rightleftharpoons Q; \; Q \rightarrow R.$$

The corresponding differential equations for Eq. 10 are

$$\frac{dR}{dt} = k_2 \cdot Q^n \qquad (11)$$

$$\frac{dQ}{dt} = k_1 \cdot C \cdot X - k_{-1} \cdot Q - nk_2 \cdot Q^n \qquad (12)$$

$$X = X_T - nQ. \qquad (13)$$

Here, X_T is the total density of X. Note that solution of Eqs. 11–13, with the steady-state assumption that $dQ/dt = 0$, leads to a saturable equation for R (see Eq. 9). Also observe that Eq. 11 now replaces the previous equation 5 for R.

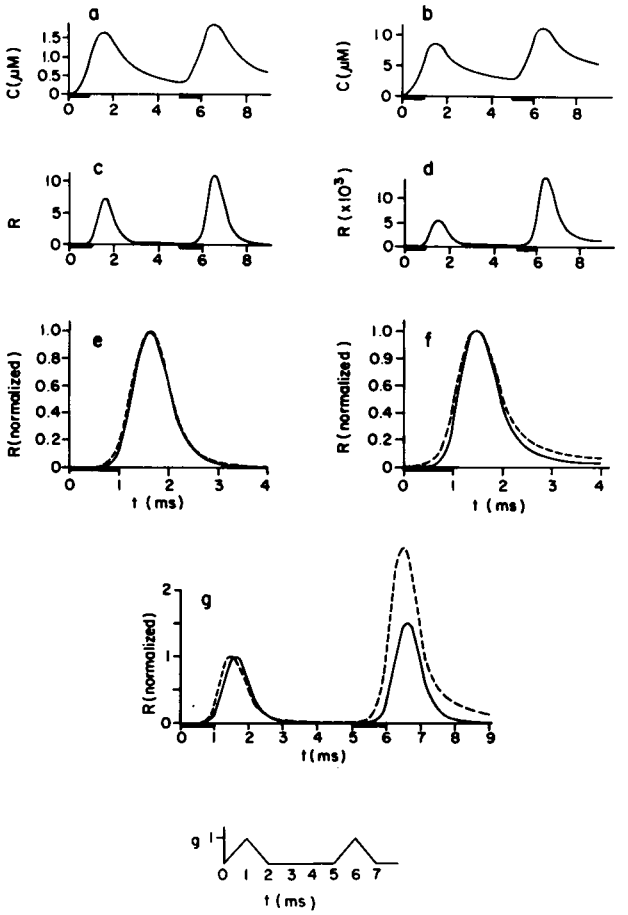

FIGURE 12 Simulation of C and R for low temperature. Conditions and details as in Fig. 9 with the difference that g rises and declines gradually (see scheme in lower part). In comparison to Fig. 9, observe that release starts later and reaches its peak after a longer delay. The difference in the duration of release is less apparent.

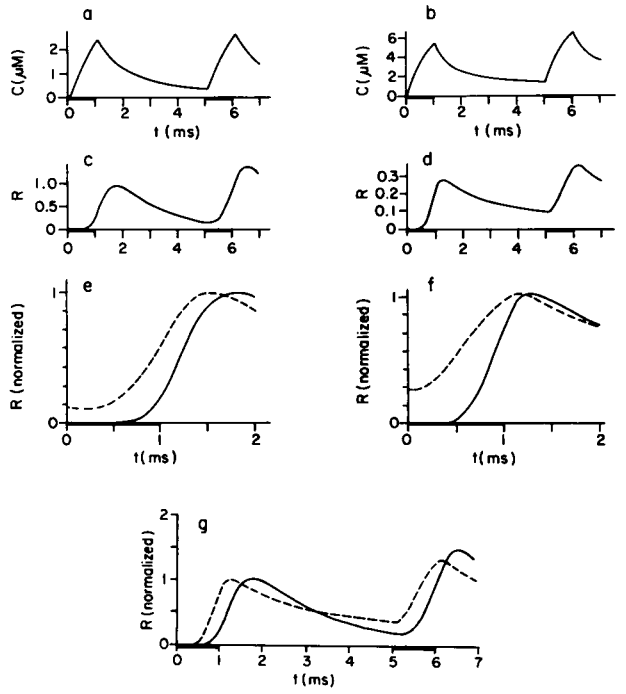

FIGURE 13 Simulations as in Fig. 9 for C, but R is calculated according to Eqs. 11–13. Parameters are $k_2 = 1\ ms^{-1}$, $k_1 = 0.5\ ms^{-1}\ \mu M^{-1}$, $k_{-1} = 0.4\ ms^{-1}$, $X_T = 1$. Note that now some of the release occurs after the pulse (i.e., in a fashion more similar to the experiments in Fig. 2). However the sensitivity of the time course of release, both on residual Ca^{2+} and on depolarizaiton, becomes even more profound.

The results of Eqs. 11–13, together with Eq. 1 for calcium, are depicted in Fig. 13. C remains unaltered (compare Fig. 13, *a* and *b*, to Fig. 9, *a* and *b*). Now, however, the fit is better between the time course of release and experimental results for a single pulse. That is, the minimal latency can be prolonged to almost outlast the pulse at the low depolarization (Fig. 13 *c*). Moreover, at the low depolarization, the peak of R, as for the experiments in Fig. 2, now significantly follows the pulse. Finally, the release process has been prolonged to last ~5 ms (Fig. 13, *c* and *d*). These improvements were made possible, because the reaction that is governed by k_2 (which eventually lumps together many steps) is now the slowest process in the chain of events leading to release. It is now this step that determines the minimal latency, and k_2 together with k_1 determine the time of the peak and the decay of the release. Neither of these rate constants describe diffusion of C. Therefore, in addition to the above listed improvements, this modified model can also provide the correct dependence of the time course of release on temperature.

Unfortunately, correcting these aspects of the 3D diffusion model worsened others. Examination of Fig. 13 shows that now the time course of release depends (even stronger than in Figs. 9, 10, and 12) on the resting level of C before stimulation. The time course of the second pulse (dashed lines, Fig. 13, *e* and *f*) is very different from that of the first. Even if the resting level before opening the channels is only $<1/10$ of the concentration that enters (see Fig. 13, *a* and *b*), it strongly affects the time course. The release elicited by the second pulse started much sooner, without any latency, and the whole time course is modified. Also, as noticed before in Figs. 9, 10, and 12, as depolarization increases, release starts and reaches its peak sooner (dashed line in Fig. 13 *g*). This prediction becomes even more pronounced now that a step subsequent to the entry of Ca^{2+} is the slowest one. Note also that in Fig. 13, as in the experiments (Fig. 2) but contrary to the unsaturated R (Fig. 9), facilitation is higher at the lower depolarization (Fig. 13 *g*).

Dependence of R on extracellular Ca^{2+} concentration

An additional test for any variation of the Ca theory is its ability to correctly predict the dependence of release on extracellular Ca^{2+} concentration. Unfortunately, the 3D diffusion model does not include a direct influx of Ca^{2+} by means of Ca^{2+} channels, and therefore, this model exhibits no direct dependence on extracellular Ca^{2+} concentration. We tried to mimic a possible dependence on extracellular Ca^{2+} concentration by keeping the f function as before, but by changing the amplitude of g while keeping its duration unaltered. This modification ensures that the time course of the influx of C will remain the same at the various levels of extracellular Ca^{+} concentration. The results are depicted in Fig. 14 *a*. Indeed, the time course of C at the higher (solid line) and the lower (dashed line) g are similar, the only difference being the amplitude of C. The resulting normalized Rs are seen in Fig. 14, *b–d*. In Fig. 14 *b*, the unsaturated R (Eq. 5) was employed, while in Fig. 14 *c*, the saturated R (Eq. 9) was used. In Fig. 14 *d*, R was obtained, as presented in Fig. 13, by solving Eqs. 11–13. The unsaturated R (Fig. 14 *b*) predicts that the time course of release is independent of extracellular Ca^{2+} concentration. This prediction agrees with experimental results; Datyner and Gage (1980) showed that the time course of release was the same at two levels of extracellular Ca^{2+} concentration. The agreement with experiments collapses, however, if the unsaturated R is replaced by the more natural saturated R (Fig. 14 *c*). Then, as concentration increases (dashed line), the rising time of R is altered, and moreover, release is prolonged. A completely different time course of release at the two levels of extracellular Ca^{2+} concentration is expected upon introduction of a slower process following the entry of Ca^{2+} (Fig. 14 *d*). Then, not only does release start earlier and last longer at the higher level of C, but also the peak is reached sooner.

DISCUSSION

For some time, academic arguments have existed as to the ability of the Ca theory to account for experimental results. We decided to study carefully and systematically what seems to be one of the most sophisticated versions of the Ca theory, the 3D diffusion model of Fogelson and Zucker (1985). These authors claim that their model can account for both the time course of release after a single pulse, and the time course of facilitation. The latter is discussed in a subsequent paper (Hovav, G., H. Parnas, and I. Parnas, manuscript in preparation). Here, we concentrate on the time course of release. It should be emphasized that our conclusions address the behavior of the time course of evoked release of a single pulse, without any ties to the origin of facilitation of a second pulse.

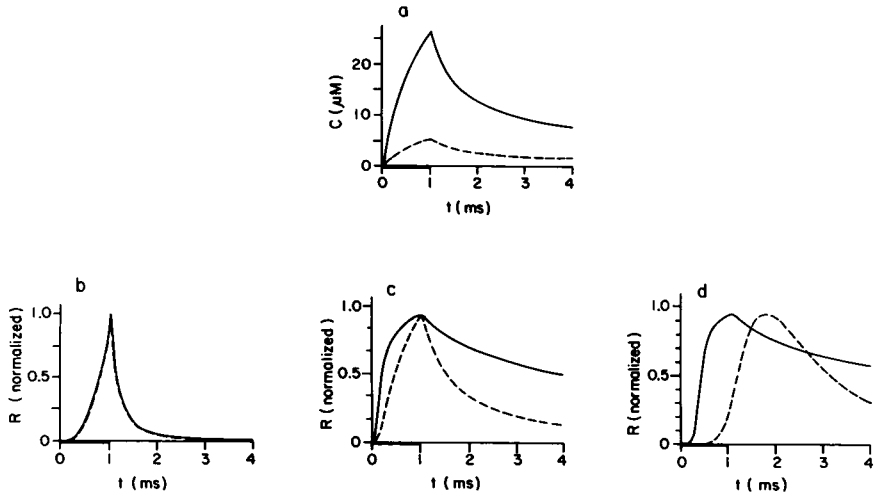

FIGURE 14 Simulation of the dependence of C and R on extracellular Ca^{2+} concentration. Variations in the extracellular Ca^{2+} concentration were simulated by changing g (see Eq. 2a). g, for the lower concentration, was taken to be 0.5, and for the higher concentration, 2.5. The high level of depolarization has been employed. The time course of C at the two concentrations is depicted in *a*. R in *b* is calculated according to Eq. 5. The values of the peak amplitudes of R are 6^4 at the lower concentration of C and 27^4 at the higher concentration. R in *c* is calculated according to Eq. 9. The values of the peak amplitudes of R are 0.32 for the low C and 0.743 for the high C. R in *d* is calculated according to Eqs. 11–13. The values of the peak amplitudes of R are 0.28 for the low C and 0.7 for the high C. The curves shown in *b–d* are the normalized Rs of the low (*dashed line*) and the high (*solid line*) concentrations of C. Note that only when R is a nonsaturating function of C do the two normalized curves of R overlap (*b*). When R saturates at higher C (*c*), or when the kinetic equations that underlie saturation (i.e., Eqs. 11–13) are employed (*d*), release starts sooner and lasts longer at the higher g.

A model, in general, must be developed to harmonize a body of experimental results. Success in predicting one result, at only one set of experimental conditions, does not show that the model is worthwhile. This is even more so when a complicated model, such as the present one, is presented. Therefore, because the 3D diffusion model claims to account for the time course of release, it is important to study it under a variety of experimental conditions. The experiments address the two key assumptions of the model: (*a*) Ca^{2+} is the only limiting factor in determining release, and (*b*) diffusion governs the time course of release.

It has been shown here that the model, as such, cannot account for many of the experimental findings. The most important aspects of the experimental results have been summarized in points *a–d* under Experimental Results. To recapitulate, release occurs mainly after the depolarizing pulse, and not during the pulse. Moreover, the time course of release is insensitive to the amplitude of depolarization, or to the level of intracellular calcium, *C*, before stimulation. In contrast, the time course of release is very sensitive to temperature.

The 3D diffusion model did not correctly predict any of these results. In particular, this model gave the following conclusions: (*a*) Most of the release occurs during the pulse, with only a decaying phase after the depolarizing pulse. (*b*) Release is sensitive to the amplitude of depolarization; release starts and reaches its peak sooner as depolarization increases. (*c*) Release is sensitive to the level of C before stimulation. It starts sooner and lasts longer as the residual level of *C* is elevated. (*d*) Release is insensitive to temperature.

In an attempt to correct predictions (*a*) and (*d*) by introducing a slow step after the entry of Ca^{2+}, or by slowing the kinetics of the Ca^{2+} channels, we found that predictions (*b*) and (*c*) contradict the experimental observations even more.

In earlier work, we have shown analytically that an unavoidable conclusion of the Ca theory is that various aspects of the time course of release must depend heavily on variations in the temporal Ca^{2+} concentration (Parnas, H., and Segel, 1984; Parnas, H., et al., 1986*a* and *b*). It could, however, be claimed that refinement of the Ca theory to include the present spatio-temporal details could diminish this dependency. To this end, we tried here to test the 3D diffusion model by choosing parameters in computer simulations so that agreement with experiment was achieved in several respects. But we could find no parameter set that gave all major qualitative features of the experiments. This, of course, does not prove that such a set does not exist. We doubt the existence of such a set, however, both because of the analytical work just mentioned and because our parameter selection was done with the aid of a good understanding of the qualitative effect of each parameter as described earlier in the text. The same reasoning makes us skeptical of the ability of other variants of the 3D diffusion model, in particular that of Simon and Llinas (1985), to account for all of the qualitative findings.

If we are correct that the 3D diffusion model fails to account for the insensitivity of the time course of release to temporal variations in C, then there is a fundamental deficiency in the model. Moreover, it also points to the source of the deficiency. For the time course of release to be insensitive to modifications in the temporal (and spatial) concentrations of Ca^{2+}, another parameter not associated with Ca^{2+} must determine the time course of release.

We have suggested (see Parnas, H., and I. Parnas, 1989) that in the neuromuscular junction, depolarization, in addition to Ca^{2+}, is required for release. Whether or not this suggestion is correct is beside the point here. Our claim is that even a highly sophisticated 3D formulation of the classical "calcium model" for neurotransmitter release cannot account for all of the major experimental facts.

We thank L. A. Segel for his help in revising the manuscript. We would also like to thank Julie Anello for editing the revised version.

This research was supported by the Goldie-Anna Charitable Trust Endowment Fund.

Received for publication 13 June 1988 and in final form 21 November 1988.

REFERENCES

Barrett, E. F., and C. F. Stevens. 1972. The kinetics of transmitter release at the frog neuromuscular junction. *J. Physiol. (Lond.).* 227:691–708.

Crank, J. 1975. The Mathematics of Diffusion. 2nd ed. Clarendon Press, Oxford.

Datyner, N. B., and P. W. Gage. 1980. Phasic secretion of acetylcholine at a mammalian neuromuscular junction. *J. Physiol. (Lond.).* 303:299–314.

Dodge, F. A., Jr., and R. Rahamimoff. 1967. Cooperative action of calcium ions in transmitter release at the neuromuscular junction. *J. Physiol. (Lond.).* 193:419–432.

Dudel, J. 1981. The effect of reduced calcium on quantal unit current and release at the crayfish neuromuscular junction. *Pfluegers Arch. Eur. J. Physiol.* 391:35–40.

Dudel, J. 1984*a*. Control of quantal transmitter release at frog's motor nerve terminals. *Pfluegers Arch. Eur. J. Physiol.* 402:225–234.

Dudel, J., I. Parnas, and H. Parnas. 1983. Neurotransmitter release and its facilitation in crayfish muscle. VI. Release determined in both intracellular calcium concentration and depolarization of the nerve terminal. *Pfluegers Arch. Eur. J. Physiol.* 339:1–10.

Fogelson, A. L., and R. S. Zucker. 1985. Presynaptic calcium diffusion from various arrays of single channels. *Biophys. J.* 48:1003–1017.

Hodgkin, A. L., and R. D. Keynes. 1957. Movement of labelled calcium in squid giant axons. *J. Physiol. (Lond.).* 138:153–281.

Katz, B., and R. Miledi. 1965*a*. The measurement of synaptic delay, and the time course of acetylcholine release at the neuromuscular junction. *Proc. R. Soc. Lond. B.* 161:483–495.

Katz, B., and R. Miledi. 1965*b*. The effect of temperature on the synaptic delay at the neuromuscular junction. *J. Physiol. (Lond.).* 181:656–670.

Katz, B., and R. Miledi. 1968. The role of calcium in neuromuscular facilitation. *J. Physiol. (Lond.).* 195:481–492.

Katz, B., and R. Miledi. 1977. Suppression of transmitter release at the neuromuscular junction. *Proc. R. Soc. Lond. B.* 196:465–469.

Llinas, R., I. Z. Steinberg, and K. Walton. 1981. Relationship between presynaptic calcium current and post-synaptic potentiation in squid synapse. *Biophys. J.* 33:332–351.

Matzner, H., H. Parnas, and I. Parnas. 1988. Presynaptic effects of d-tubocurarine on neurotransmitter release at the neuromuscular junction of the frog. *J. Physiol. (Lond.).* 398:109–121.

Miledi, R. 1973. Transmitter release induced by injection of calcium ions into nerve terminals. *Proc. R. Soc. Lond. B.* 183:421–425.

Parnas, H., and I. Parnas. 1987. Influence of depolarization pulse duration on the time course of transmitter release in lobster. *J. Physiol. (Lond.).* 388:487–494.

Parnas, H., and I. Parnas. 1989. New perspectives on the role of Ca^{2+} and voltage in neurotransmitter release. *In* Presynaptic Regulation of Neurotransmitter Release. A. Handbook, J. J. Feigenbaum, and M. Hanani, editors. Freund Publishing Ltd., Tel Aviv. In press.

Parnas, H., and L. A. Segel. 1980. A theoretical explanation for some effects of calcium on the facilitation of neurotransmitter release. *J. Theor. Biol.* 84:3–29.

Parnas, H., and L. A. Segel. 1984. Exhaustion of calcium does not terminate evoked neurotransmitter release. *J. Theor. Biol.* 107:345–365.

Parnas, H., J. Dudel, and I. Parnas. 1982. Neurotransmitter release and its facilitation in crayfish. I. Saturation kinetics of release and of entry and removal of calcium. *Pfluegers Arch. Eur. J. Physiol.* 393:1–14.

Parnas, H., J. Dudel, and I. Parnas. 1986*a*. Neurotransmitter release and its facilitation in crayfish. VII. Another voltage dependent process beside Ca entry controls the time course of phasic release. *Pfluegers Arch. Eur. J. Physiol.* 406:121–130.

Parnas, H., I. Parnas, and L. Segel. 1986*b*. A new method for determining co-operativity in neurotransmitter release. *J. Theor. Biol.* 119:481–499.

Parnas, I., and H. L. Atwood. 1966. Phasic and tonic neuromuscular systems in the abdominal extensor muscles of the crayfish and lobster. *Comp. Biochem. Physiol.* 18:701–723.

Parnas, I., and H. Parnas. 1986. Calcium is essential but insufficient for neurotransmitter release: the Calcium-voltage hypothesis. Gif lectures in neurobiology, regulation of synaptic plasticity. *J. Physiol. (Paris).* 81:289–305.

Parnas, I., and H. Parnas. 1988. The "Ca-Voltage" hypothesis for neurotransmitter release. *Biophys. Chem.* 29:85–93.

Parnas, I., H. Parnas, and J. Dudel. 1986. Neurotransmitter release and its facilitation in crayfish. VIII. Modulation of release by hyperpolarizing pulse. *Pfluegers Arch. Eur. J. Physiol.* 406:131–137.

Simon, S. M., and R. Llinas. 1985. Compartmentalization of the submembrane calcium activity during calcium influx and its significance in transmitter release. *Biophys. J.* 48:485–498.

Stockbridge, N., and J. W. Moore. 1984. Dynamics of intracellular calcium and its possible relationship to phasic transmitter release and facilitation at the frog neuromuscular junction. *J. Neurosci.* 4:803–811.

Wojtowicz, J. M., I. Parnas, H. Parnas, and H. L. Atwood. 1987. Latency of transmitter release at crayfish motor nerve endings examined by intracellular depolarization. *Can. J. Physiol. Pharmacol.* 65:105–108.

Zucker, R. S., and A. L. Fogelson. 1986. Relationship between transmitter release and presynaptic calcium influx when calcium enters through discrete channels. *Proc. Natl. Acad. Sci. USA.* 83:3032–3036.